THE JOURNAL OF PHYSICAL CHEMISTRY B

ARTICLE

pubs.acs.org/JPCB

Increasing the Exchange Time-Scale That Can Be Probed by CPMG Relaxation Dispersion NMR

Pramodh Vallurupalli,[†] Guillaume Bouvignies,[†] and Lewis E. Kay[†,‡,*]

[†]Departments of Molecular Genetics, Biochemistry, and Chemistry, The University of Toronto, Toronto, Ontario M5S 1A8, Canada

[‡]Program in Molecular Structure and Function, Hospital for Sick Children, 555 University Avenue, Toronto, Ontario M5G 1X8, Canada

Supporting Information

ABSTRACT: Carr−Purcell−Meiboom−Gill relaxation dispersion NMR spectroscopy has emerged as a valuable tool to characterize conformational exchange between major and minor states in a large variety of biomolecules. The window of exchange that is amenable for study, corresponding to rates on the order of 2000 s^{-1} or less, is limiting, however. Here we show that a combined analysis of both amide ^{15}N and $^{1}H^{N}$ CPMG profiles and major state exchange induced ^{15}N chemical shift changes leads to significant increases in the exchange time scale for which accurate exchange parameters and chemical shift differences between the interconverting states can be obtained. The utility of the approach is illustrated with examples involving a pair of protein systems that are in the moderately fast exchange regime. In these cases the analysis of dispersion profiles alone is not sufficient to obtain robust measures of exchange parameters and chemical shift differences. Inclusion of major state exchange induced ^{15}N chemical shift changes measured in ($^{15}N-^{1}H^{N}$) HMQC and HSQC data sets in addition to the ^{15}N and $^{1}H^{N}$ dispersion profiles in the analysis "breaks" the correlation in parameters, allowing accurate values to be obtained. The approach is straightforward to implement and makes use of HMQC/HSQC data sets that are recorded as a matter of routine to obtain chemical shifts of the excited state. It promises to increase the range of exchanging systems involving low populated, transiently formed excited states that can be studied by relaxation dispersion NMR.

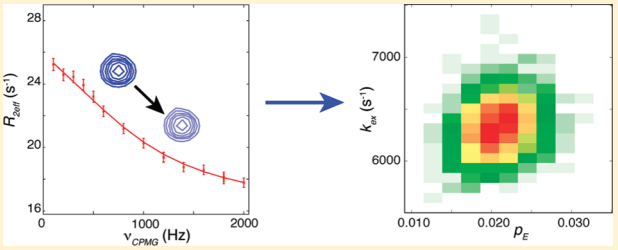

INTRODUCTION

Solution NMR spectroscopy has become an established technique for obtaining high quality structures of biomolecules (<30−40 kDa) and for characterizing the interactions between these molecules and their targets.[1−3] However, such studies provide a necessarily incomplete picture for understanding the relation between structure, dynamics and function because they focus only on highly populated (ground state) conformers that can be readily accessed. Low populated and transiently formed structures (so-called excited states) that have been shown to play important roles in biological function[4−7] remain invisible to standard approaches so that relatively little is known about them. The situation is changing, however, with the continued development[8−10] of Carr−Purcell−Meiboom−Gill[11,12] (CPMG) relaxation dispersion NMR spectroscopy. Here effective transverse relaxation rates, $R_{2,eff}$, are quantified as a function of the delay (τ) between variable numbers of refocusing pulses that are applied during a relaxation interval.[8,13] Fits of $R_{2,eff}(\nu_{CPMG}=1/(2\tau))$ to an appropriate model of chemical exchange allow the extraction of the kinetic and thermodynamic parameters that govern the exchange process as well as the absolute values of the chemical shift differences between ground and excited states ($|\Delta\omega|$ in rad/s, $|\Delta\varpi|$ in ppm) so long as the excited states are populated to at least 0.5% and exchange with the ground conformer with rates, k_{ex}, between ∼100 and ∼2000 s^{-1}.[8,14] Separation of kinetics, thermodynamics, and chemical shift parameters remains only possible, however, if at least some of the exchanging spins are not in the fast exchange regime corresponding to $k_{ex}/\Delta\omega \rightarrow \infty$ (hence $k_{ex} <$ ∼2000 s^{-1}).

In cases where chemical shifts of the excited state are obtained, they can be used as sensitive probes of structure, especially when combined with database programs such as CS-Rosetta,[15] Cheshire,[16] or CS23D.[17] For example, we have recently shown in a number of applications that atomic resolution structures of "invisible" excited protein states can be generated using chemical shift restraints, supplemented in some cases by residual dipolar couplings and chemical shift anisotropies, which are measured exclusively from relaxation dispersion experiments.[4,18,19] It is clear that such experiments can be very powerful. However, at present the exchange time-scale window for which the methodology is applicable is limiting because, as mentioned above, k_{ex} values must be less than approximately 2000 s^{-1}. Here we show that a combined analysis of relaxation

Received: October 5, 2011
Revised: October 13, 2011
Published: November 11, 2011

dispersion data sets (i.e., transverse relaxation rates) and exchange induced shifts of major state peak positions leads to an increase in the exchange time scale over which the full set of exchange parameters can be extracted. A theoretical description is provided that explains how this comes about. Subsequently, the utility of this approach is demonstrated experimentally for a triple mutant of T4 lysozyme (L99A, G113A,R119P T4L) exchanging with a rate, k_{ex}, of approximately 6000 s^{-1} at 20 °C, for which accurate chemical shift differences and populations of the exchanging states could not be obtained from fits of dispersion profiles alone. In contrast, the combined analysis of chemical shifts and relaxation rates described here facilitate the accurate extraction of $\Delta\tilde{\omega}$ values. The range of applicability of this methodology is then further established from studies on a relatively fast folding mutant of the FF domain from HYPA/FBP11,[20] where it is shown that even in cases approaching the moderately fast exchange regime ($k_{ex}/\Delta\omega \sim 3-4$, 18.8T), robust estimates of shifts are still possible.

MATERIALS AND METHODS

NMR Samples. $^{15}N,^{13}C,^{1}H$ L99A,G113A,R119P T4L was prepared as described previously.[19] The resulting NMR sample was ~1.5 mM in protein dissolved in 50 mM sodium phosphate, 25 mM NaCl, 2 mM EDTA, 2 mM NaN_3 pH 5.5, 10% D_2O buffer. An $^{15}N,^{13}C,^{1}H$ I44A,V67A FF domain sample was prepared as before.[4] The sample conditions where ~1.5 mM protein, 50 mM sodium acetate, 100 mM NaCl, pH 5.7 10% D_2O buffer.

NMR Experiments. Experiments were performed on Varian Inova spectrometers (11.7 and 18.8T) equipped with room temperature triple resonance probes. $^{1}H^{N}$ CPMG relaxation dispersion experiments were recorded at both 11.7 and 18.8T for the FF domain sample and only at 18.8T for the T4L sample, whereas ^{15}N CPMG dispersion profiles and HSQC and HMQC data sets were measured at both 11.7 and 18.8T for both proteins. Most of the experiments involving T4L were performed at 20.5 °C ($k_{ex} \sim 6000\ s^{-1}$) whereas additional dispersion data used to obtain reference chemical shift differences were collected at 15 °C ($k_{ex} \sim 3900\ s^{-1}$). Temperatures were calibrated using a thermocouple that was inserted into the magnet in a standard NMR tube.

^{15}N CPMG relaxation dispersion data sets were recorded using a constant-time (CT) version[13] of the relaxation compensated TROSY CPMG pulse sequence.[21] The CT CPMG period, T_{relax}, was set to 24 (30 ms) for L99A,G113A,R119P T4L (I44A, V67A FF domain). $^{1}H^{N}$ dispersion profiles were recorded using a standard CT relaxation compensated pulse scheme[22] (FF domain) or a CT sequence that does not include relaxation compensation and where magnetization originates as antiphase with respect to the coupled nitrogen (T4L). Such a scheme was chosen for T4L to eliminate any ROE derived cross-peaks in spectra arising from cross-relaxation in the rotating frame; such peaks are more pronounced in larger proteins (T4L is over a factor of 2 larger than the FF domain and experiments on T4L were performed at a lower temperature). T_{relax} values of 18 and 20 ms were used for L99A,G113A,R119P T4L and the I44A, V67A FF domain, respectively. Partial refocusing of the evolution of $^{1}H^{N}-^{1}H$ scalar couplings during the CPMG relaxation period in amide proton relaxation experiments was achieved using an $^{1}H^{N}$ band selective REBURP pulse[23] applied in the center of the CPMG period.[22]

Relaxation dispersion experiments were recorded as a series of 2D planes with interleaved ν_{CPMG} values (~15), with 2−3 repeats to estimate errors. ν_{CPMG} values ranged from ~50−1000 Hz for ^{15}N dispersions and up to 2000 Hz in the $^{1}H^{N}$ dispersion experiments. Typically, each complete dispersion data set was recorded in 15−28 h.

Complementary high resolution $^{1}H^{N}$,^{15}N HSQC and HMQC spectra were recorded using previously published pulse sequences.[24] Maximum t_1 evolution periods were 76.8 (74) and 102.4 (100) ms at 11.7 (18.8)T for the T4 and the FF domain samples, respectively. Experiments were recorded two or three times to estimate the errors in peak positions.

Data Processing and Analysis. All NMR spectra were processed using the NMRPipe software package,[25] with visualization and analysis achieved using Sparky.[26] Peak intensities were extracted using the program FuDA (http://pound.med.utoronto.ca/software.html) and effective relaxation rates, $R_{2,eff}$, subsequently calculated according to the relation[27]

$$R_{2,\mathrm{eff}}(\nu_{\mathrm{CPMG}}) = -\frac{1}{T_{\mathrm{relax}}}\ln\left(\frac{I(\nu_{\mathrm{CPMG}})}{I_{\mathrm{o}}}\right) \quad (1)$$

In eq 1 I_o is the intensity of a peak in the reference spectrum recorded without the CPMG relaxation delay and $I(\nu_{CPMG})$ is the corresponding peak intensity in the spectrum measured at a frequency of ν_{CPMG}.

^{15}N ($^{1}H^{N}$) dispersion profiles from the FF domain were included in the analysis described below so long as $R_{2,eff}(\nu_{CPMG}=0,18.8T) - R_{2,eff}(\nu_{CPMG}\rightarrow\infty,18.8T) > 1.5\ s^{-1}$ ($3\ s^{-1}$). Criteria for inclusion of data from T4L are as described previously.[19] In cases where both ^{15}N and $^{1}H^{N}$ dispersion profiles were included in fits (so that $\Delta\tilde{\omega}(^{15}N) \neq 0$ and $\Delta\tilde{\omega}(^{1}H^{N}) \neq 0$) values of $\tilde{\omega}_{SQ} - \tilde{\omega}_{MQ}$ were also added.

Global exchange parameters, k_{ex} and p_E, along with residue specific values for $\Delta\tilde{\omega}$ and the intrinsic transverse relaxation rates $R_{2,eff}(\nu_{CPMG}\rightarrow\infty)$ were obtained by minimization of a χ^2 function

$$\chi^2 = \sum_{i=1}^{N}\frac{(M_i^{\mathrm{exp}} - M_i^{\mathrm{calc}})^2}{\sigma_i} \quad (2)$$

using an in-house written program that is available upon request. In eq 2 M_i^{exp} is an experimentally measured relaxation or shift value ($R_{2,eff}(\nu_{CPMG})$ or $\tilde{\omega}_{SQ} - \tilde{\omega}_{MQ}$), M_i^{calc} is the corresponding calculated value, σ_i is the error in the experimental measurement estimated from repeat experiments, and the summation is over all (N) experimental data points. Values of $R_{2,eff}(\nu_{CPMG})$ were calculated by solving the Bloch−McConnell equations[28] as a function of k_{ex}, p_E, $\Delta\tilde{\omega}$, and $R_{2,eff}(\nu_{CPMG}\rightarrow\infty)$ assuming ideal refocusing pulses and a two-state exchange process. Chemical shift differences, $\tilde{\omega}_{SQ} - \tilde{\omega}_{MQ}$, were obtained by diagonalization of the Bloch−McConnell exchange matrix with the peak positions of the exchanging states given by the complex part of the eigenvalues that are obtained with $\Delta\tilde{\omega} = \Delta\tilde{\omega}_N$ (HSQC) or by averaging over shifts calculated with $\Delta\tilde{\omega} = \Delta\tilde{\omega}_N \pm \Delta\tilde{\omega}_H$ (HMQC).

In total (12,12,10), (12,30,9), (6,12,3) ^{15}N, $^{1}H^{N}$ dispersion profiles and $\tilde{\omega}_{SQ} - \tilde{\omega}_{MQ}$ values were included in the analysis for L99A,G113A,R119P T4L (out of a total of 160 non-Pro residues in the protein), I44A,V67A FF (all data; 68 non-Pro residues in the protein), and I44A,V67A FF ($\Delta\tilde{\omega}(^{15}N) < 3.5$ ppm or $\Delta\tilde{\omega}(^{1}H^{N}) < 0.35$ ppm; 39 non-Pro residues), respectively;

reduced χ^2 values of 0.7, 0.9, and 0.7 were obtained in the fits, providing confidence in the simple two-state exchange model that has been used in the analysis. As the exchange time scale increases toward fast exchange and dispersion profiles approach linearity, the validity of the two-state approximation does become more difficult to substantiate, unless exchange rates in a multistep fast exchange process are significantly different.[29] In the present study we have restricted ν_{CPMG} to $\leq$1 kHz (^{15}N) and 2 kHz (^{1}H^{N}); however, higher values can be used that will further increase the deviation from linearity, improving the accuracy of extracted k_{ex} values and allowing for a better assessment of the efficacy of two-state fits of the data.

Errors in the fitted parameters were estimated using a standard bootstrap procedure[30] whereby a set of 2000 data sets was generated from the original experimental data. Each new data set was created in the following way. All k $R_{2,eff}(\nu_{CPMG})$ values in the original data set were assigned a number between 1 and k, a random number p was selected such that $1 \leq p \leq k$, and data point p was retained in the new data matrix. A similar procedure was employed for the $\tilde{\omega}_{SQ} - \tilde{\omega}_{MQ}$ values. In this manner a data set is obtained with the same number of experimental points as the original parent (same number of $R_{2,eff}(\nu_{CPMG})$ and $\tilde{\omega}_{SQ} - \tilde{\omega}_{MQ}$values) but where any original value can be represented several times or left out. Each of the 2000 bootstrap sets were fit, as the original data, and the distribution of k_{ex}, p_E, $\Delta\tilde{\omega}$ and $R_{2,eff}(\nu_{CPMG}\rightarrow\infty)$ values used to estimate errors and to establish whether robust parameters could be obtained from the experimental data. All calculations were carried out on the GPC supercomputer of the SciNet HPC consortium with each bootstrap calculation (2000 data sets) taking approximately two hours.

RESULTS AND DISCUSSION

Correlation between Exchange Parameters as the Exchange Time Scale Increases. The underlying goal in relaxation dispersion NMR studies of exchanging protein systems is to extract accurate values of exchange rates, populations of exchanging states and chemical shift differences between nuclei in the interconverting ground (G) and excited (E) conformations.[9] In the case of a two-site exchange process, $G \underset{k_{EG}}{\overset{k_{GE}}{\rightleftharpoons}} E$, this corresponds to the global parameters, $k_{ex} = k_{GE} + k_{EG}$ and the population of the excited state, p_E (=1 − p_G), as well as $\Delta\omega_{EG} = \omega_E - \omega_G$ where ω_j is the chemical shift of a nucleus in state j ($j \in \{E,G\}$), and intrinsic relaxation rates for each exchanging spin.

The chemical shifts of the excited state resonances are of particular interest to our laboratory because these can be used to obtain detailed structural information. To improve the accuracy of the extracted parameters, dispersion profiles are typically recorded at a number of static magnetic fields.[4,18,19] Because chemical shift differences scale linearly with the magnetic field, the exchange time scale is modulated; residues with large $k_{ex}/\Delta\omega$ values at low magnetic field, and hence in the "fast" exchange regime, are "slowed down" by performing the experiment at higher magnetic field (smaller $k_{ex}/\Delta\omega$). Ideally, an exchanging system should comprise nuclei with a distribution of $k_{ex}/\Delta\omega$ values, with many in the range 0−2.

Figure 1A shows such a distribution for the L99A cavity mutant of T4 lysozyme (L99A T4L) that exchanges between ground and excited states, 25 °C,[19,31] with the global exchange parameters p_E and k_{ex} obtained from a bootstrap analysis of the dispersion profiles plotted in Figure 1B (see Materials and Methods). Both ^{15}N[21,32] and ^{1}H^{N}[22] profiles recorded at static magnetic field strengths of 11.7 and 18.8T are included in the analysis. It is clear that well-defined values of (p_E, k_{ex}) are obtained, centered about (3.54%, 1300 s^{-1}), consistent with expectations based on the underlying $k_{ex}/\Delta\omega$ profile. Not surprisingly, precise values of $\Delta\tilde{\omega}$ are also obtained, as shown for I29 in Figure 1C (^{15}N, 3.79 ± 0.05 ppm).

In contrast, the situation is different in the case of a triple mutant of T4 lysozyme, L99A,G113A,R119P T4L, which interconverts approximately 4-fold faster than L99A T4L at 20 °C. Here the distribution of $k_{ex}/\Delta\omega$ values is decidedly shifted to larger values, Figure 1D (compare with Figure 1A), and the corresponding (p_E, k_{ex}) distribution is much less well-defined, with p_E values extending from 0 to 50% (values greater than 50% are not allowed in the minimization process), Figure 1E. Precise residue specific $\Delta\tilde{\omega}$ values can no longer be isolated from fits of dispersion profiles, with $\Delta\tilde{\omega}$ correlated strongly with p_E (see below), as shown in Figure 1F for $\Delta\tilde{\omega}$(^{15}N) of I29.

The difficulties with extracting robust measures of p_E and $\Delta\omega$ as the exchange time-scale increases are well documented in the literature. For example, Luz and Meiboom showed close to 50 years ago that in the fast exchange ($k_{ex}/\Delta\omega > 10$), slow pulsing ($\nu_{CPMG} < 0.1\ k_{ex}$) limit, $R_{2,eff}(\nu_{CPMG})$ varies as[33]

$$R_{2,\mathrm{eff}}(\nu_{CPMG}) = \left(1 - 4\frac{\nu_{CPMG}}{k_{ex}}\right)\frac{p_G p_E (\Delta\omega)^2}{k_{ex}} + R_{2,\mathrm{eff}}(\nu_{CPMG} \rightarrow \infty) \quad (3)$$

Even when $R_{2,eff}(\nu_{CPMG}\rightarrow\infty)$ can be estimated accurately, p_E (or p_G) and $\Delta\omega$ remain coupled, precluding extraction of accurate chemical shift differences.

For exchanging systems that are not in the "true" fast regime, such as L99A,G113A,R119P T4L where $k_{ex}/\Delta\omega$ values are $\geq$1.9 (with the majority 3−4 or greater, but less than 10, Figure 1D), it is still difficult to obtain accurate values of p_E and $\Delta\omega$ from fits of dispersion profiles exclusively, Figures 1E,F, even when reasonably accurate k_{ex} values can be fit. One approach might be to record additional dispersion data sets at a higher static magnetic field strength that effectively increases $\Delta\omega$ so that the ratio $k_{ex}/\Delta\omega$ is decreased; in the case of L99A,G113A,R119P T4L the values of $k_{ex}/\Delta\omega$ in Figure 1D are for 18.8T, currently the highest field available to us so that this is not an option. A second approach involves manipulation of k_{ex} through temperature, for example. In cases where the exchange process involves large activation enthalpies, it may be possible to decrease k_{ex} so that it falls within the ∼100−2000 s^{-1} window that is generally amenable for CPMG studies. However, in many systems this is not possible. The goal in these cases becomes, therefore, to break the correlation between p_E and $\Delta\omega$ by an additional measurement that depends on the exchange parameters differently than transverse relaxation rates. We have recently shown through simulation that a combined analysis of relaxation dispersion profiles and chemical shift data obtained by a divided evolution (D-evolution) experiment[34] in which peak positions in spectra shift as the effective exchange time regime is varied could be used to obtain robust measures of exchange parameters in cases of slow chemical exchange[35] (k_{ex} values on the order of 20−50 s^{-1}). In this limit there is a pronounced correlation between p_E and

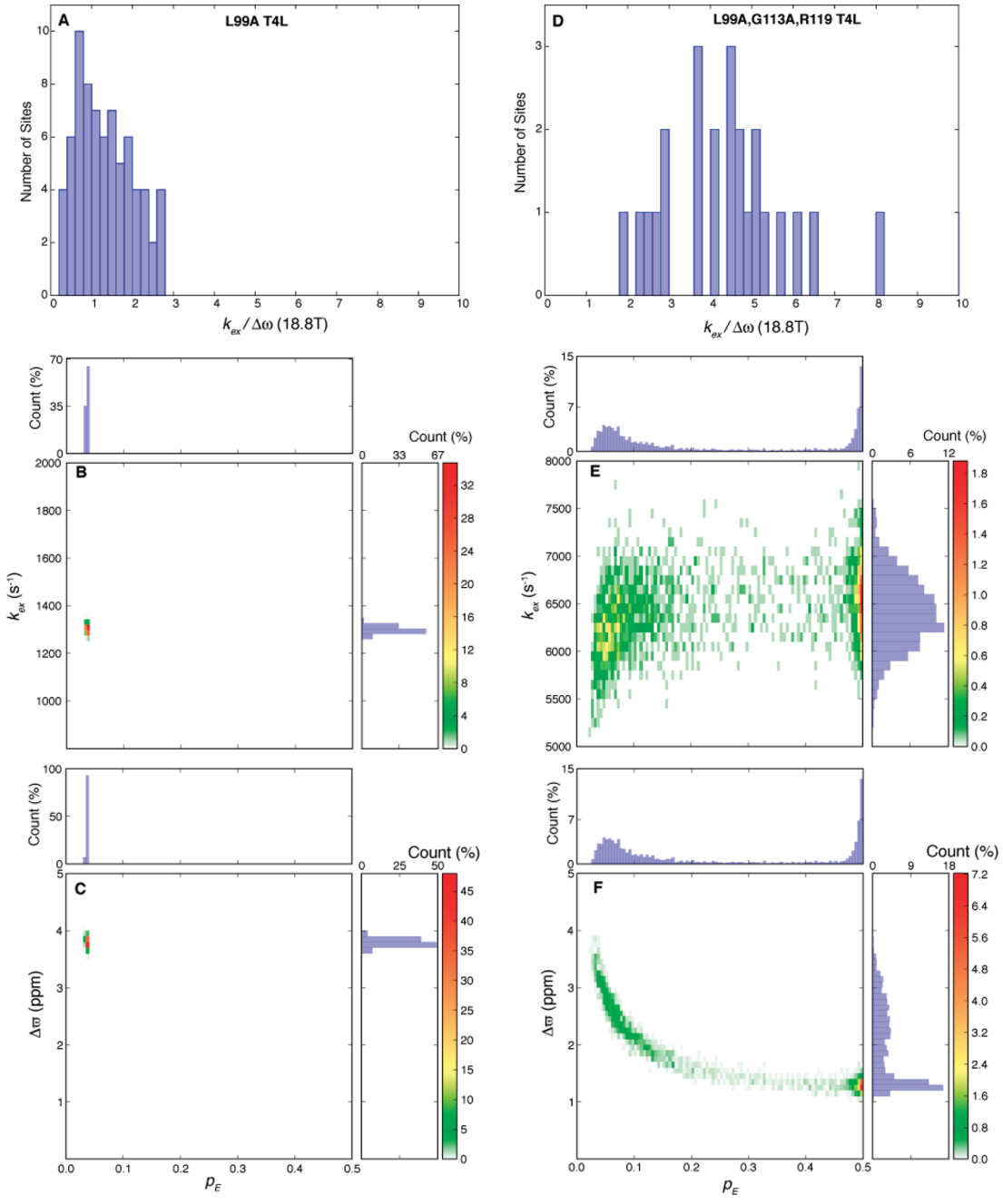

Figure 1. As the exchange time scale increases, the exchange parameters extracted from CPMG relaxation dispersion data become less well-defined. (A) Histogram showing the distribution of $k_{ex}/\Delta\omega$ values (18.8T) for ^{15}N and $^{1}H^{N}$ nuclei of L99A T4L, 25 °C. Only values ≤10 are shown. The distribution extends over a wide range of values, with many residues in slow-intermediate exchange. (B) Distribution of (p_E, k_{ex}) values, centered at (3.54 ± 0.04%, 1300 ± 20 s^{-1}), obtained from a bootstrap analysis of ^{15}N and $^{1}H^{N}$ CPMG relaxation dispersion data sets recorded at 11.7 and 18.8T. Each bin of the two-dimensional histogram is colored according to the fraction of points that lie in it and projected along *X* (above) or *Y* (right-hand side) axes; the fraction of points in each bin can be read from the scale on the axis at the far right. (C) Distribution of (p_E, $\Delta\tilde{\omega}$) for Ile 29 obtained from the bootstrap fit of the dispersion data. (D)−(F) correspond to (A)−(C) but for the protein L99A,G113A,R119P T4L, 20 °C, which interconverts between ground and excited states with a rate approximately 4-fold faster than L99A T4L. Note that it is no longer possible to define either p_E (E) or $\Delta\tilde{\omega}$ (F) values from simultaneous fits of ^{15}N and $^{1}H^{N}$ CPMG relaxation dispersion data sets recorded at 11.7 and 18.8T.

k_{ex} in fits of either dispersion data sets or D-evolution chemical shift profiles alone. Such a divided evolution scheme cannot be used in cases of moderately fast exchange, considered here, because prohibitively high radio frequency pulsing rates would be required to shift peak positions. We show below, however, that a combined quantitative analysis of relaxation dispersion profiles and ground state chemical shifts measured as a function of static magnetic field or as a comparison of peak positions recorded in HMQC/HSQC data sets facilitates the extraction of accurate values of p_E and $\Delta\omega$ that are otherwise coupled for systems that exchange in the moderately fast regime.

dx.doi.org/10.1021/jp209610v |*J. Phys. Chem. B* 2011, 115, 14891–14900

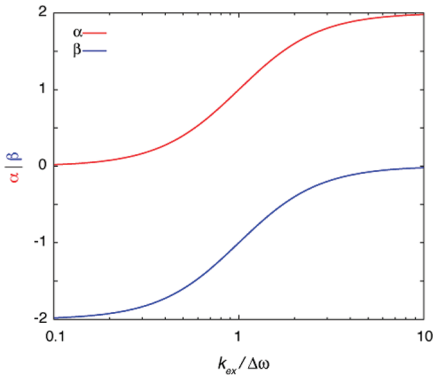

Figure 2. Chemical exchange induced broadening (red) and shift (blue) of the major state peak scale differently with static magnetic field strength. Plots of the parameters α and β as a function of $k_{ex}/\Delta\omega$, calculated using eqs 8 and 9, respectively.

Consider a nucleus attached to a system undergoing conformational exchange between states G and E, $G \underset{k_{EG}}{\overset{k_{GE}}{\rightleftharpoons}} E$, as described above, with $p_E \ll 1$. In this limit expressions for exchange broadening, R_{ex}, and for the exchange induced shift of the observable line, δ_{ex}, are given by

$$R_{ex} = k_{GE}\frac{\frac{\Delta R_{EG}}{k_{ex}}\left(1+\frac{\Delta R_{EG}}{k_{ex}}\right)+\left(\frac{\Delta\omega_{EG}}{k_{ex}}\right)^2}{\left(1+\frac{\Delta R_{EG}}{k_{ex}}\right)^2+\left(\frac{\Delta\omega_{EG}}{k_{ex}}\right)^2} \quad (4)$$

$$\delta_{ex} = k_{GE}\frac{\left(\frac{\Delta\omega_{EG}}{k_{ex}}\right)}{\left(1+\frac{\Delta R_{EG}}{k_{ex}}\right)^2+\left(\frac{\Delta\omega_{EG}}{k_{ex}}\right)^2} \quad (5)$$

where $\Delta R_{EG} = R_E - R_G$ and R_i is the intrinsic relaxation rate of $i \in \{E, G\}$. Equations similar to these have been derived previously,[24] but the present relations are slightly more accurate for $|k_{ex}/\Delta\omega| \sim 2$ that is of interest in the studies considered here where the exchange time scale is between intermediate and fast. In this limit and assuming further that $\Delta R_{EG} = 0$, eqs 4 and 5 simplify as follows,

$$R_{ex} \approx p_E\Delta\omega_{EG}\left(\frac{\Delta\omega_{EG}}{k_{ex}}\right)\left(1-\left(\frac{\Delta\omega_{EG}}{k_{ex}}\right)^2\right) \quad (6)$$

$$\delta_{ex} \approx p_E\Delta\omega_{EG}\left(1-\left(\frac{\Delta\omega_{EG}}{k_{ex}}\right)^2\right) \quad (7)$$

and the different dependencies of R_{ex} and δ_{ex} on $\Delta\omega_{EG}$, k_{ex} is made clear. The differential dependence of relaxation rates and chemical shifts on exchange parameters can be further appreciated by considering expressions for how these vary as a function of magnetic field strength. Millet et al. have shown[36] that assuming $\Delta R_{EG} = 0$

$$\frac{d\ln R_{ex}}{d\ln B_o} = \alpha = \frac{2\left(\frac{k_{ex}}{\Delta\omega_{EG}}\right)^2}{1+\left(\frac{k_{ex}}{\Delta\omega_{EG}}\right)^2} \quad (8)$$

In a similar manner, starting from eq 5, it follows that

$$\frac{d\ln\tilde{\delta}_{ex}}{d\ln B_o} = \beta = \frac{-2}{1+\left(\frac{k_{ex}}{\Delta\omega_{EG}}\right)^2} \quad (9)$$

where $\tilde{\delta}_{ex}$ is the exchange induced shift of the ground state peak measured in ppm and B_o is the static magnetic field. Figure 2 plots α and β as a function of $k_{ex}/\Delta\omega$. As discussed previously,[36] α varies between 0 (slow exchange) and 2 (fast exchange) and provides a measure of the exchange time scale; in contrast, β ranges from -2 in the slow exchange limit to 0 in fast exchange. For small changes in B_o (from $B_o - \Delta B$ to $B_o + \Delta B$) it follows directly from eqs 8 and 9 that

$$R_{ex}(B_o+\Delta B) = \left(\frac{B_o+\Delta B}{B_o-\Delta B}\right)^{\alpha}R_{ex}(B_o-\Delta B) \quad (10)$$

$$\tilde{\delta}_{ex}(B_o+\Delta B) = \left(\frac{B_o+\Delta B}{B_o-\Delta B}\right)^{\beta}\tilde{\delta}_{ex}(B_o-\Delta B) \quad (11)$$

where $\Delta\omega$ in α and β is evaluated for a static field of B_o. Equations 10 and 11 establish that the static field dependencies of R_{ex} and $\Delta\tilde{\delta}_{ex}$ are very different because α and β depend on the exchange parameters in different ways. Previously, Skrynnikov et al. showed that it is possible to obtain the signs of $\Delta\omega$ and hence the chemical shifts of the excited state by qualitative comparison of ground state chemical shifts recorded at two or more static magnetic fields, $\Delta\tilde{\delta}_{ex}$, or by comparing chemical shifts obtained from single and multiple-quantum data sets, $\tilde{\omega}_{SQ} - \tilde{\omega}_{MQ}$.[24] The above discussion suggests, however, that $\Delta\tilde{\delta}_{ex}$ or $\tilde{\omega}_{SQ} - \tilde{\omega}_{MQ}$ can be even more useful. Because chemical shifts and relaxation rates are influenced differently by chemical exchange, a combined quantitative fit of dispersion profiles and $\Delta\tilde{\delta}_{ex}$ or $\tilde{\omega}_{SQ} - \tilde{\omega}_{MQ}$ values provides an avenue for separating exchange parameters that would otherwise be correlated as the exchange time scale increases.

Breaking the Correlation by Combining Relaxation Dispersion Data and $\Delta\tilde{\delta}_{ex}$ or $\tilde{\omega}_{SQ} - \tilde{\omega}_{MQ}$. We have carried out a combined fit of ^{15}N and $^{1}H^{N}$ relaxation dispersion profiles and $\tilde{\omega}_{SQ} - \tilde{\omega}_{MQ}$ values recorded on the L99A,G113A,R119P T4L exchanging system at 11.7 and 18.8T, 20 °C. As described above, fits of the relaxation dispersion data exclusive of $\Delta\tilde{\delta}_{ex}$ or $\tilde{\omega}_{SQ} - \tilde{\omega}_{MQ}$ resulted in a broad distribution of (p_E, k_{ex}) values and ill defined chemical shift differences between exchanging states. In contrast, the combined fit (see Materials and Methods for details) results in much better defined global exchange parameters, Figure 3A (compare with Figure 1E). Not surprisingly, excellent agreement is obtained between calculated and experimental $\tilde{\omega}_{SQ} - \tilde{\omega}_{MQ}$, Figure 3B, because these values were used in the fit. Although it is clear that much more precise values of exchange parameters are obtained in the combined analysis of Figure 3A, the accuracy of these parameters, including the extracted chemical shift differences, $\Delta\tilde{\omega}$, must be established. In this regard L99A,G113A,R119P T4L is a particularly good system to evaluate our methodology because the exchange rate can be significantly manipulated by small changes in temperature and it is this property in particular that prompted us to use it as a model system for part of this work (see below). As discussed above, however, there are many exchanging systems for which such manipulations are not possible and where the exchange regime is moderately fast over the range of temperatures that can

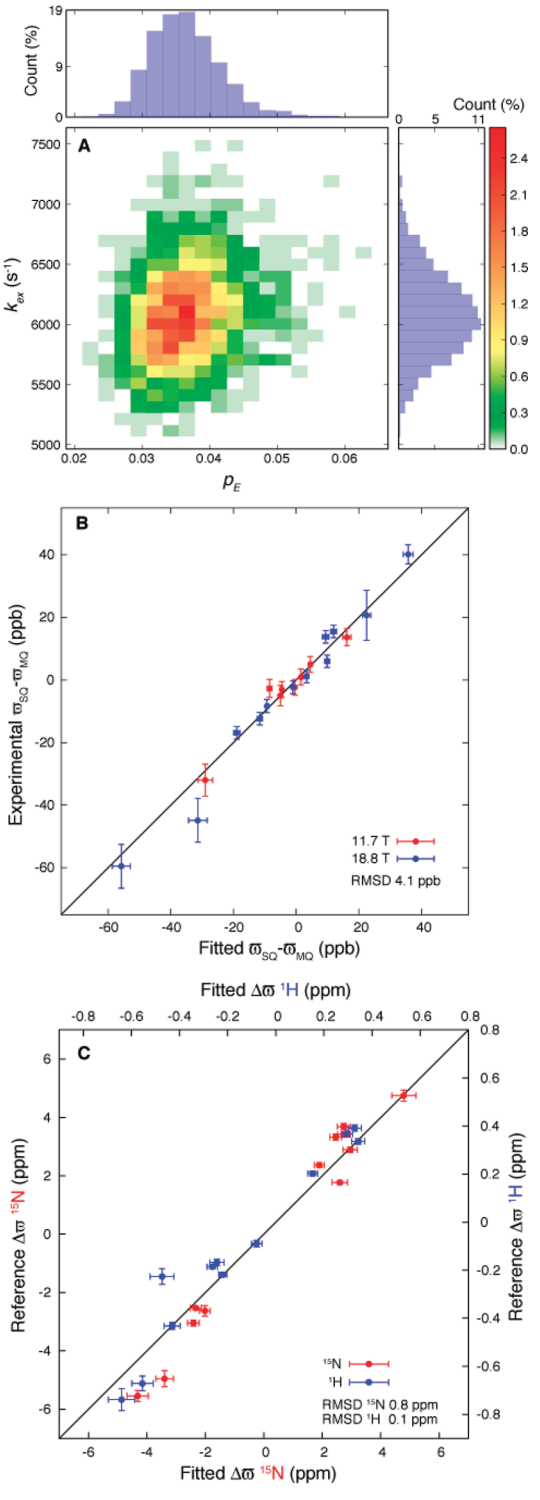

Figure 3. Simultaneous fits of CPMG relaxation dispersion data and $\tilde{\omega}_{SQ} - \tilde{\omega}_{MQ}$ values lead to robust estimates of p_E and $\Delta\tilde{\omega}$ values for L99A,G113A, R119P T4L, 20 °C. (A) (p_E, k_{ex}) distribution (centered at (3.6 ± 0.6%, 6100 ± 350 s^{-1})) obtained from a combined bootstrap analysis of $^1H^N$ and ^{15}N CPMG data and $\tilde{\omega}_{SQ} - \tilde{\omega}_{MQ}$ values, establishing that both k_{ex} and p_E can be determined very precisely. As in Figure 1, each bin of the two-dimensional histogram is colored according to the fraction of points that lie in it. (B) Linear correlation plot of measured and calculated $\tilde{\omega}_{SQ} - \tilde{\omega}_{MQ}$ values. (C) Fitted ^{15}N and $^1H^N$ $\Delta\tilde{\omega}$ values are in good agreement with reference chemical shift differences obtained from an analysis of CPMG relaxation dispersion data recorded at 15 °C where k_{ex} is smaller (~3870 s^{-1} relative to ~6100 s^{-1}).

be reasonably studied. For these systems it is not possible to extract meaningful $\Delta\tilde{\omega}$ values or exchange parameters and the methodology presented here becomes critical.

Figure 3C shows that a good correlation is obtained between the ^{15}N and $^1H^N$ $\Delta\tilde{\omega}$ values extracted from the combined fit (X-axis) and the corresponding reference $\Delta\tilde{\omega}$ values (Y-axis). Here the reference shifts were obtained from fits of relaxation dispersion data sets recorded at a lower temperature (15 °C) where k_{ex} is appreciably smaller (3870 ± 100 s^{-1} vs 6100 ± 350 s^{-1}) so that accurate values could be obtained using the dispersion data exclusively. The small deviations between $^{15}N/^1H^N$ $\Delta\tilde{\omega}$ values in the correlation plot of Figure 3C cannot be attributed to the differences in the temperatures (20 and 15 °C) at which the dispersion experiments were performed because amide temperature coefficients are on the order of 0−10 ppb/K for $^1H^N$ (average of 18 ppb/K for ^{15}N measured in uqibuitin).[37−39] Rather, they most likely reflect errors in the measurements themselves. In any event these errors are well within the accuracy of predicted $^{15}N/^1H^N$ shifts from structure[40] so that the excited state chemical shifts obtained from them can be used reliably as restraints in structural studies.

It is worth re-emphasizing that as the exchange time scale approaches the fast limit the terms in the product $p_E p_G \Delta\omega^2$ (see eq 3) cannot be separated. Thus, for $p_G \sim 1$, as in the examples considered here, the extracted value of $\Delta\omega_e$ is related to the correct value, $\Delta\omega_c$, by

$$\Delta\omega_c = \sqrt{\frac{p_E^e}{p_E^c}}\Delta\omega_e \qquad (12)$$

where p_E^e and p_E^c are the fitted and the actual (correct) values of the excited state population, respectively. The fact that accurate $\Delta\omega$ values are obtained by the combined relaxation/shift analysis (Figure 3C) indicates that an accurate p_E value has also been isolated from the fit (Figure 3A).

As a final note, we have also recorded $\Delta\tilde{\delta}_{ex}$ values in the hope of using these to break the correlation between p_E and $\Delta\omega$. Whereas combined fits of dispersion and $\Delta\tilde{\delta}_{ex}$ data do indeed show that p_E and $\Delta\omega$ are no longer coupled, the correlation between calculated and experimental $\Delta\tilde{\delta}_{ex}$ values was not as good as the corresponding plot in Figure 3B that is based on $\tilde{\omega}_{SQ} - \tilde{\omega}_{MQ}$ values. Of course, values of $\Delta\tilde{\delta}_{ex}$ are obtained from measurements at a pair of magnetic fields and it is critical that parameters, such as sample temperature, be adjusted to be as close as possible for each experiment. Small temperature variations between different instruments is the likely explanation for the difference in quality of the $\Delta\tilde{\delta}_{ex}$ and $\tilde{\omega}_{SQ} - \tilde{\omega}_{MQ}$ correlations described above. In this context we have noted in an application involving another exchanging protein system that even a very modest (0.2 °C) temperature miscalibration between spectrometers can lead to a noticeable change in $\Delta\tilde{\delta}_{ex}$ (Supporting Information Figure 1). Because $\tilde{\omega}_{SQ} - \tilde{\omega}_{MQ}$ is obtained as a difference based on measurements recorded on the same spectrometer, this is much less of an issue, even when values at multiple magnetic fields are used. For this reason we favor chemical shift data from HMQC/HSQC measurements in fits with the relaxation dispersion curves, although for obtaining signs of $\Delta\omega$, where only a qualitative analysis is required, both $\Delta\tilde{\delta}_{ex}$ and $\tilde{\omega}_{SQ} - \tilde{\omega}_{MQ}$ are extremely useful.[24]

Range of Applicability. Results from the L99A,G113A,R119P T4L exchanging system clearly show the utility of simultaneously fitting transverse relaxation rates and $\tilde{\omega}_{SQ} - \tilde{\omega}_{MQ}$ values. As a

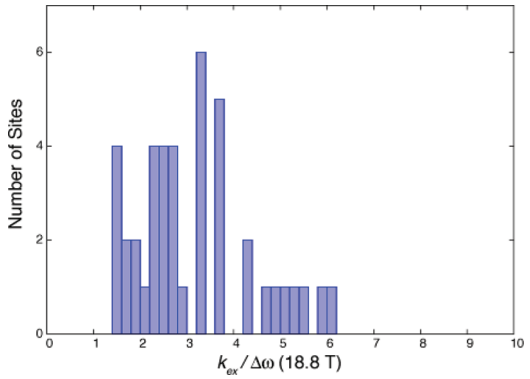

Figure 4. Histogram showing the distribution of $k_{ex}/\Delta\omega$ values (18.8 T) for ^{15}N and ^{1}H^{N} sites of the I44A,V67A FF domain. Only values $\leq$10 are shown. Although k_{ex} is substantial ($\sim$ 5650 s^{-1}), $\Delta\omega$ values can be large in this exchanging system so that a minimum $k_{ex}/\Delta\omega$ of $\sim$1.4 is obtained.

further illustration, we have used a second protein system, the I44A,V67A FF domain,[20] that exchanges between an on-pathway folding intermediate and the folded state with $k_{ex} \sim 5700$ s^{-1}, 36 °C. Although the interconverting states of the FF domain share many structural features there are also some very significant differences[4] leading to large $\Delta\tilde{\omega}$ values. For example, $\Delta\tilde{\omega}(^{15}\text{N}) >$ 4 ppm for four residues whereas $\Delta\tilde{\omega}(^{1}\text{H}^{N}) >$ 0.4 ppm at 17 sites. As a result, the $k_{ex}/\Delta\omega$ distribution is not as skewed as it might otherwise be, Figure 4, certainly much less than for the L99A, G113A,R119P T4L system. For example, in contrast to T4L where $k_{ex}/\Delta\omega < 2$ and $2< k_{ex}/\Delta\omega < 3$ at only one and 4 sites, respectively, for the FF domain there are 8 and 14 sites within these ranges. The increased uniformity in and the larger distribution of $k_{ex}/\Delta\omega$ values for the FF domain translates into more robust fitted exchange parameters.

Not surprisingly, therefore, when ^{15}N and ^{1}H^{N} dispersion data recorded at 11.7 and 18.8T are fitted together (without $\tilde{\omega}_{SQ} - \tilde{\omega}_{MQ}$), well-defined ($p_E$,$k_{ex}$) values are obtained, Figure 5A, centered at (2.1%, 5660 s^{-1}). The importance of dispersion data recorded at a pair of static magnetic fields is made clear by the fact that the exchange parameters are less well-defined when profiles recorded at 18.8T alone are fit, Figure 5B. In this case, by recording data over a range of magnetic fields the exchange time scales for some of the residues are varied, as those with large $\Delta\omega$ values are in the moderately slow exchange regime at higher field (18.8T), whereas they are shifted to faster exchange at lower field (11.7T). Thus, complementary information is obtained from the two-field data sets. Notably, if all residues were already in the moderately fast exchange time scale at 18.8T, then shifting to lower field would have provided no new information. When the dispersion profiles recorded at 18.8T are fit together with ^{15}N $\tilde{\omega}_{SQ} - \tilde{\omega}_{MQ}$ values (also recorded at 18.8T, inset to Figure 5C), a well-defined (p_E,k_{ex}) distribution is obtained, Figure 5C. The center of this distribution is at (2.2%, 5700 s^{-1}), much like for the case when dispersion data sets recorded at 18.8T and 11.7T were analyzed simultaneously (Figure 5A). Thus, the "orthogonal" information content of dispersion data and $\tilde{\omega}_{SQ} - \tilde{\omega}_{MQ}$ values parallels in some sense that in dispersion profiles recorded at multiple fields. Moreover, this result suggests that, when only a single static magnetic field is available for measurements, a combined analysis of dispersion profiles and exchanged induced chemical shift differences can provide reasonable estimates of (p_E, k_{ex}) values.

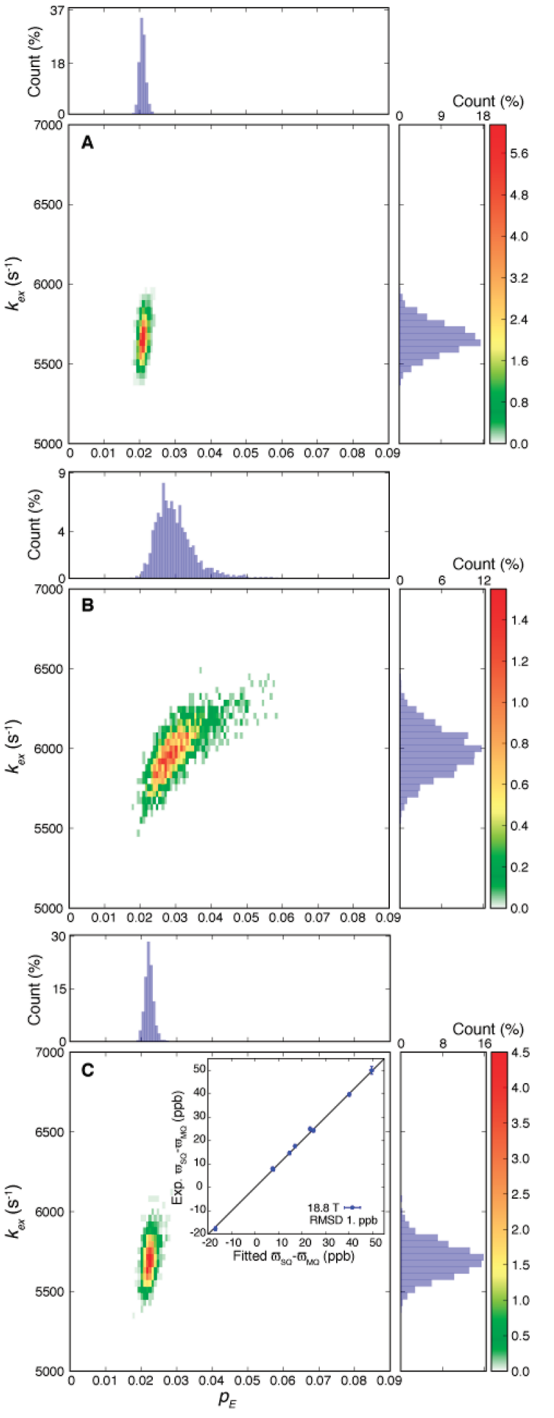

Figure 5. Values of $\tilde{\omega}_{SQ} - \tilde{\omega}_{MQ}$ are complementary to CPMG transverse relaxation rates. (A) Bootstrap analysis of ^{15}N and ^{1}H^{N} dispersion profiles recorded on the I44A,V67A FF domain (11.7, 18.8T), 36 °C. A well-defined (p_E, k_{ex}) distribution (centered at (2.1 $\pm$ 0.1%, 5660 $\pm$ 100 s^{-1})) is generated that is in contrast with that obtained when only the 18.8T data are included in the analysis (B). (C) Combined fits of the 18.8T dispersion data and $\tilde{\omega}_{SQ} - \tilde{\omega}_{MQ}$ values significantly increase the precision of the (p_E, k_{ex}) distribution ((p_E, k_{ex}) = (2.2 $\pm$ 0.1%, 5700 $\pm$ 100 s^{-1}). Shown in the inset is a linear correlation plot of experimental and fitted $\tilde{\omega}_{SQ} - \tilde{\omega}_{MQ}$ values. Details of the histograms in the figure are as per Figures 1 and 3.

It should be emphasized that $\tilde{\omega}_{SQ} - \tilde{\omega}_{MQ}$ values are readily measured and are necessary for obtaining the signs of

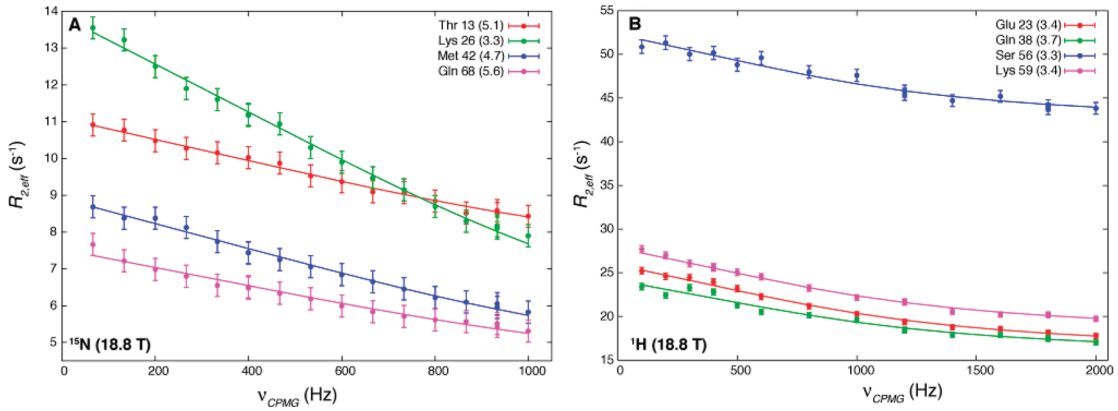

Figure 6. ^{15}N (A) and $^{1}H^{N}$ (B) CPMG relaxation dispersion profiles are shown for selected residues from the I44A,V67A FF domain, 18.8T, 36 °C. Residues chosen are those for which the smallest $k_{ex}/\Delta\omega$ ratios are obtained in a restricted data set where $\Delta\tilde{\omega}$ (^{15}N) < 3.5 ppm or $\Delta\tilde{\omega}(^{1}H^{N})$ < 0.35 ppm (corresponding to the slowest exchanging nuclei in the data set). Values of $k_{ex}/\Delta\omega$ are shown in parentheses in the upper right-hand corner of each panel.

heteronuclear $\Delta\tilde{\omega}$ values, where they are interpreted qualitatively, along with $\Delta\delta_{ex}$.[24] Using $\tilde{\omega}_{SQ} - \tilde{\omega}_{MQ}$ values in a quantitative sense, as we have done here, thus requires no additional measurements, although, because they depend on both $\Delta\tilde{\omega}(^{15}N)$ and $\Delta\tilde{\omega}(^{1}H^{N})$, $^{1}H^{N}$ dispersions must be recorded in addition to ^{15}N profiles. This is done as a matter of course in studies of exchanging systems in our laboratory.

To assess the exchange time-scale range over which accurate exchange parameters can be extracted, we next eliminated all I44A,V67A FF domain dispersion profiles derived from residues with $\Delta\tilde{\omega}(^{15}N)$ > 3.5 ppm or $\Delta\tilde{\omega}(^{1}H^{N})$ > 0.35 ppm. In the resulting data set only residues with $k_{ex}/\Delta\omega \geq 3.3$ remain, a lower limit that is significantly larger than in the other examples considered to this point, providing a more stringent test of the methodology. Dispersion profiles for the four residues with the smallest $k_{ex}/\Delta\omega$ values (corresponding to the sites with the slowest exchange time-scales) are shown in Figure 6, with $k_{ex}/\Delta\omega$ for each indicated in the upper right-hand corner. Note that all of the ^{15}N curves are linear, as expected in cases of moderately fast exchange and relatively slow pulsing (eq 3). In contrast, the $^{1}H^{N}$ dispersions were obtained with ν_{CPMG} values up to 2 kHz (relative to 1 kHz for ^{15}N) and the profiles show some deviation from linearity that is critical for the extraction of accurate k_{ex} values, as least in cases where $R_{2,eff}(\nu_{CPMG}\rightarrow\infty)$ rates are not known from other experiments.[41,42]

Fits of the subset of ^{15}N and $^{1}H^{N}$ dispersion profiles with $\Delta\tilde{\omega}(^{15}N)$ < 3.5 ppm or $\Delta\tilde{\omega}(^{1}H^{N})$ < 0.35 ppm did not produce accurate values of (p_E, k_{ex}), as can be clearly seen in Figure 7A. The majority of extracted p_E values are approximately 0.5, which is an artifact of the fitting program. In contrast, when $\tilde{\omega}_{SQ} - \tilde{\omega}_{MQ}$ values are included, the fits converge and well-defined global exchange parameters are obtained, (p_E, k_{ex}) = (2.1 ± 0.3%, 6330 ± 220 s^{-1}), Figure 7B, that are in reasonably good agreement with those extracted from the complete set of dispersion profiles (2.1 ± 0.1%, 5660 ± 100 s^{-1}), Figure 5A. Notably, only three sets of $\tilde{\omega}_{SQ} - \tilde{\omega}_{MQ}$ values have been used: those from residues Asn 33, Met 42, and Gln 66 (11.7 and 18.8T) that are at least 3 ppb in size, ranging up to approximately 8 ppb. Because nonzero $\tilde{\omega}_{SQ} - \tilde{\omega}_{MQ}$ values are only possible when $\Delta\tilde{\omega}(^{15}N) \neq 0$ and $\Delta\tilde{\omega}(^{1}H^{N}) \neq 0$, it is necessary that both ^{15}N and $^{1}H^{N}$ dispersion profiles show a ν_{CPMG} dependence. Although only three residues satisfy these criteria, inset to Figure 7C, it is sufficient in this case to extract reasonably accurate values for both p_E (Figure 7B) and $\Delta\tilde{\omega}$ (Figure 7C, where the reference values are those from the complete dispersion data set that comprises all residues including those with $\Delta\tilde{\omega}(^{15}N)$ > 3.5 ppm or $\Delta\tilde{\omega}(^{1}H^{N})$ > 0.35 ppm). The small but systematic overestimate in the extracted $\Delta\tilde{\omega}(^{15}N)$ and $\Delta\tilde{\omega}(^{1}H^{N})$ values (maximum of 0.32 and 0.022 ppm, respectively) results from the overestimation of k_{ex} by approximately 10% when only the subset of dispersion profiles is fitted. These errors are well within the tolerance of chemical shift prediction programs[40] and would not be problematic in structural studies of excited protein states.

We have also extended our analysis to a further subset of residues where $\Delta\tilde{\omega}(^{15}N)$ < 3.0 ppm or $\Delta\tilde{\omega}(^{1}H^{N})$ < 0.30 ppm, corresponding to a $k_{ex}/\Delta\omega$ distribution that has a minimum value of 4.3. In this case, however, $\tilde{\omega}_{SQ} - \tilde{\omega}_{MQ}$ from only a single residue could be used and it was not possible to extract meaningful exchange parameters or chemical shift differences.

Uniqueness of the Measurements. As a final note it is of interest to compare the methodology presented here with $R_{1\rho}$ measurements that have traditionally been used to study exchanging systems interconverting on a time scale that is more rapid than that amenable to a "standard" CPMG analysis. In this exchange regime $R_{1\rho}$ dispersion profiles are fit to extract k_{ex} and per-residue values, $\Phi = p_G p_E(\Delta\omega)^2$. Populations and chemical shift differences are thus correlated, as discussed above in connection with the extraction of parameters from CPMG data in this limit. When k_{ex} is less than approximately 2000 s^{-1}, it has been shown experimentally, building on the elegant theoretical studies of Palmer and co-workers,[43] that it is possible to extract robust exchange parameters and chemical shifts from a series of off-resonance $R_{1\rho}$ measurements using weak spin lock fields.[44−46] In this exchange window, of course, similar information is available from analysis of CPMG dispersion curves, with the exception that unlike the $R_{1\rho}$ profiles that are sensitive to the sign of the chemical shift difference, only the absolute value of $\Delta\omega$ can be extracted from fits of CPMG data. To our knowledge, separation of chemical shifts and populations using any type of $R_{1\rho}$ experiment (on- or off-resonance) for systems with exchange properties similar to those studied here (k_{ex} on the order of 6000 s^{-1} or larger) has not been demonstrated experimentally. In any event it is quite

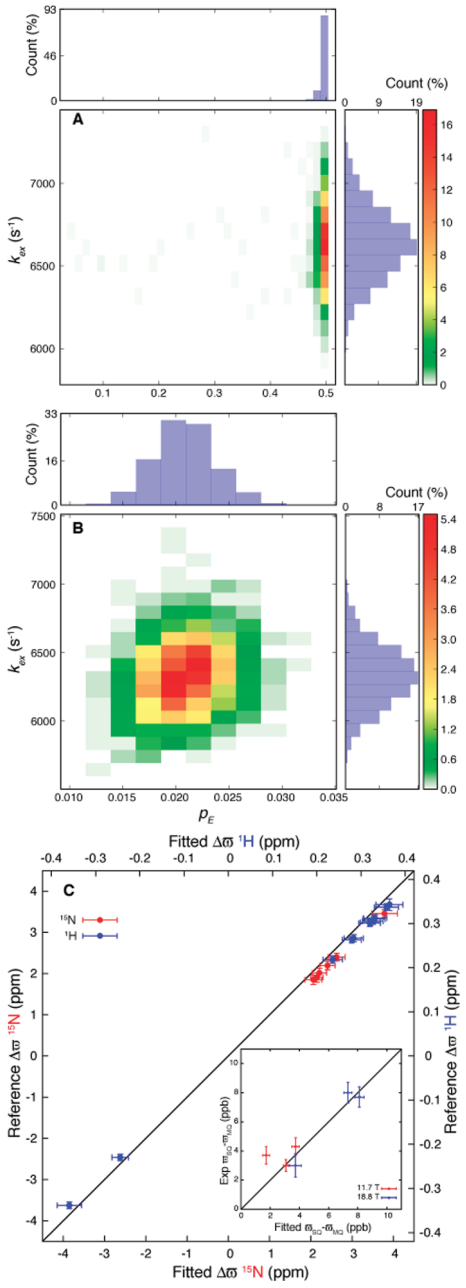

Figure 7. Excited state chemical shift values and p_E can be extracted from combined fits of dispersion data sets and $\tilde{\omega}_{SQ} - \tilde{\omega}_{MQ}$, even under conditions of moderately fast exchange. (A) Bootstrap analysis of ^{15}N, $^1H^N$ CPMG relaxation dispersion data (11.7, 18.8T) from a subset of residues in the I44A,V67A FF domain, 36 °C. ^{15}N ($^1H^N$) data were included only if $\Delta\tilde{\omega}(^{15}N) < 3.5$ ppm ($\Delta\tilde{\omega}(^1H^N) < 0.35$ ppm), so that a minimum in the $k_{ex}/\Delta\omega$ distribution (18.8T) of 3.3 is obtained. (A) The dispersion data alone are not sufficient to define p_E. (B) In contrast, addition of even a modest number of $\tilde{\omega}_{SQ} - \tilde{\omega}_{MQ}$ points (inset to C) leads to a much better defined (p_E, k_{ex}) distribution ($2.1 \pm 0.3\%$, $6330 \pm 220\ s^{-1}$) as compared with ($2.1 \pm 0.1\%$, $5660 \pm 100\ s^{-1}$) when all data are included, irrespective of $\Delta\tilde{\omega}(^{15}N)$, $\Delta\tilde{\omega}(^1H)$. (C) $\Delta\tilde{\omega}$ values from the combined dispersion, $\tilde{\omega}_{SQ} - \tilde{\omega}_{MQ}$ analysis for the subset of residues with $k_{ex}/\Delta\omega(18.8T) \geq 3.3$ are in reasonably good agreement with the reference chemical shift differences that were obtained when all of the CPMG data were included in the fits (that defines p_E, Figure 5A). As in Figures 1, 3, and 5, each bin of the two-dimensional histogram is colored according to the fraction of points that lie in it.

clear that the strategy of recording simple HMQC/HSQC data sets to resolve the correlation is much more straightforward and significantly less time-consuming.

CONCLUDING REMARKS

We have shown that a combined quantitative analysis of both transverse relaxation rates and exchange induced chemical shifts can extend the window for which accurate exchange parameters can be obtained by CPMG relaxation dispersion NMR spectroscopy. The utility of this approach has been investigated for L99A, G113A,R119P T4L that is in the moderately fast exchange regime, $k_{ex}/\Delta\omega > \sim 2$ for all residues (18.8T; median $k_{ex}/\Delta\omega = 4.4$ for all sites considered) for which accurate exchange parameters could not be extracted from analysis of multiple-field dispersion data (11.7, 18.8T) alone. Addition of $\tilde{\omega}_{SQ} - \tilde{\omega}_{MQ}$ values, however, leads to accurate estimates for p_E and $\Delta\omega$. The analysis has also been extended to the I44A,V67A FF domain. Fits of dispersion data sets from a subset of residues with $k_{ex}/\Delta\omega > 3.3$ (18.8T) yielded well-defined parameters only when supplemented with $\tilde{\omega}_{SQ} - \tilde{\omega}_{MQ}$ values. Additional analyses on data sets that include only residues exchanging on faster time scales suggest that, at least in cases when data up to 18.8T are analyzed, a lower bound of approximately 3−4 for $k_{ex}/\Delta\omega$ is required. Because measurements of $\tilde{\omega}_{SQ} - \tilde{\omega}_{MQ}$ are performed routinely to obtain signs of $\Delta\omega$, the approach does not require additional experiment time and is easily implemented in the data fitting procedure. This methodology extends the upper limit of the exchange time scale that is amenable for study, increasing the number of exchanging systems that can be analyzed by the CPMG relaxation dispersion methodology as well as the robustness of the extracted exchange parameters.

ASSOCIATED CONTENT

Supporting Information. One figure showing the sensitivity of $\Delta\tilde{\delta}_{ex}$ values to small changes in temperature between spectrometers, focusing on the FF domain exchanging system. This material is available free of charge via the Internet at http://pubs.acs.org.

AUTHOR INFORMATION

Corresponding Author

*E-mail: Kay@pound.med.utoronto.ca. Ph: 416-978-0741. Fax: 416-978-6885.

ACKNOWLEDGMENT

We thank Prof. Julie Forman-Kay for providing laboratory space and Dr. Tomasz Religa for producing the FF domain sample. We thank Dr. Patrik Lundstrom (Linköping University), Dr. Dmitry Korzhnev (University of Connecticut), and Dr. Flemming Hansen (UCL) for useful discussions. G.B. acknowledges The Canadian Institutes of Health Research (CIHR) for a postdoctoral fellowship. L.E.K. holds a Canada Research Chair in Biochemistry. This work was supported by grants from the CIHR and the Natural Sciences and Engineering Research Council of Canada, with computations performed on the GPC supercomputer at the SciNet HPC Consortium.

REFERENCES

(1) Wüthrich, K. *NMR of Proteins and Nucleic Acids*; John Wiley & Sons: New York, 1986.
(2) Zuiderweg, E. R. *Biochemistry* **2002**, *41*, 1–7.
(3) Clore, G. M.; Gronenborn, A. M. *Science* **1991**, *252*, 1390–1399.
(4) Korzhnev, D. M.; Religa, T. L.; Banachewicz, W.; Fersht, A. R.; Kay, L. E. *Science* **2010**, *329*, 1312–1316.
(5) Boehr, D. D.; McElheny, D.; Dyson, H. J.; Wright, P. E. *Science* **2006**, *313*, 1638–1642.
(6) Fraser, J. S.; Clarkson, M. W.; Degnan, S. C.; Erion, R.; Kern, D.; Alber, T. *Nature* **2009**, *462*, 669–673.
(7) Ishima, R.; Freedberg, D. I.; Wang, Y. X.; Louis, J. M.; Torchia, D. A. *Struct. Fold Des.* **1999**, *7*, 1047–1055.
(8) Palmer, A. G.; Kroenke, C. D.; Loria, J. P. *Methods Enzymol.* **2001**, *339*, 204–238.
(9) Korzhnev, D. M.; Kay, L. E. *Acc. Chem. Res.* **2008**, *41*, 442–451.
(10) Hansen, D. F.; Vallurupalli, P.; Kay, L. E. *J Biomol. NMR* **2008**, *41*, 113–120.
(11) Carr, H. Y.; Purcell, E. M. *Phys. Rev.* **1954**, *54*, 630–638.
(12) Meiboom, S.; Gill, D. *Rev. Sci. Instrum.* **1958**, *29*, 688–691.
(13) Tollinger, M.; Skrynnikov, N. R.; Mulder, F. A. A.; Forman-Kay, J. D.; Kay, L. E. *J. Am. Chem. Soc.* **2001**, *123*, 11341–11352.
(14) Korzhnev, D. M.; Salvatella, X.; Vendruscolo, M.; Di Nardo, A. A.; Davidson, A. R.; Dobson, C. M.; Kay, L. E. *Nature* **2004**, *430*, 586–590.
(15) Shen, Y.; Lange, O.; Delaglio, F.; Rossi, P.; Aramini, J. M.; Liu, G.; Eletsky, A.; Wu, Y.; Singarapu, K. K.; Lemak, A.; et al. *Proc. Natl. Acad. Sci. U. S. A.* **2008**, *105*, 4685–4690.
(16) Cavalli, A.; Salvatella, X.; Dobson, C. M.; Vendruscolo, M. *Proc. Natl. Acad. Sci. U. S. A.* **2007**, *104*, 9615–9620.
(17) Wishart, D. S.; Arndt, D.; Berjanskii, M.; Tang, P.; Zhou, J.; Lin, G. *Nucleic Acids Res.* **2008**, *36*, W496–502.
(18) Vallurupalli, P.; Hansen, D. F.; Kay, L. E. *Proc. Natl. Acad. Sci. U. S. A.* **2008**, *105*, 11766–11771.
(19) Bouvignies, G.; Vallurupalli, P.; Hansen, D. F.; Correia, B. E.; Lange, O.; Bah, A.; Vernon, R. M.; Dahlquist, F. W.; Baker, D.; Kay, L. E. *Nature* **2011**, *477*, 111–114.
(20) Jemth, P.; Day, R.; Gianni, S.; Khan, F.; Allen, M.; Daggett, V.; Fersht, A. R. *J. Mol. Biol.* **2005**, *350*, 363–78.
(21) Loria, J. P.; Rance, M.; Palmer, A. G. *J. Biomol. NMR* **1999**, *15*, 151–155.
(22) Ishima, R.; Torchia, D. *J. Biomol. NMR* **2003**, *25*, 243–248.
(23) Geen, H.; Freeman, R. *J. Magn. Reson.* **1991**, *93*, 93–141.
(24) Skrynnikov, N. R.; Dahlquist, F. W.; Kay, L. E. *J. Am. Chem. Soc.* **2002**, *124*, 12352–12360.
(25) Delaglio, F.; Grzesiek, S.; Vuister, G. W.; Zhu, G.; Pfeifer, J.; Bax, A. *J. Biomol. NMR* **1995**, *6*, 277–293.
(26) Goddard, T. D.; Kneller, D. *SPARKY*, Version 3.114; University of California: San Fransisco, CA, 2008.
(27) Mulder, F. A. A.; Skrynnikov, N. R.; Hon, B.; Dahlquist, F. W.; Kay, L. E. *J. Am. Chem. Soc.* **2001**, *123*, 967–975.
(28) McConnell, H. M. *J. Chem. Phys.* **1958**, *28*, 430–431.
(29) Grey, M. J.; Wang, C. Y.; Palmer, A. G. *J. Am. Chem. Soc.* **2003**, *125*, 14324–14335.
(30) Press, W. H.; Flannery, B. P.; Teukolsky, S. A.; Vetterling, W. T. *Numerical Recipes in C*; Cambridge University Press: Cambridge, U.K., 1988.
(31) Mulder, F. A. A.; Mittermaier, A.; Hon, B.; Dahlquist, F. W.; Kay, L. E. *Nat. Struct. Biol.* **2001**, *8*, 932–935.
(32) Vallurupalli, P.; Hansen, D. F.; Stollar, E. J.; Meirovitch, E.; Kay, L. E. *Proc. Natl. Acad. Sci. U. S. A.* **2007**, *104*, 18473–18477.
(33) Luz, Z.; Meiboom, S. *J. Chem. Phys.* **1963**, *39*, 366–370.
(34) Zhuravleva, A.; Orekhov, V. Y. *J. Am. Chem. Soc.* **2008**, *130*, 3260–3261.
(35) Bouvignies, G.; Hansen, D. F.; Vallurupalli, P.; Kay, L. E. *J. Am. Chem. Soc.* **2011**, *133*, 1935–1945.
(36) Millet, O.; Loria, J. P.; Kroenke, C. D.; Pons, M.; Palmer, A. G. *J. Am. Chem. Soc.* **2000**, *122*, 2867–2877.
(37) Cierpicki, T.; Otlewski, J. *J. Biomol. NMR* **2001**, *21*, 249–261.
(38) Farber, P.; Darmawan, H.; Sprules, T.; Mittermaier, A. *J. Am. Chem. Soc.* **2010**, *132*, 6214–6222.
(39) Bouvignies, G.; Vallurupalli, P.; Cordes, M. H.; Hansen, D. F.; Kay, L. E. *J. Biomol. NMR* **2011**, *50*, 13–18.
(40) Shen, Y.; Bax, A. *J. Biomol. NMR* **2010**, *48*, 13–22.
(41) Hansen, D. F.; Yang, D.; Feng, H.; Zhou, Z.; Wiesner, S.; Bai, Y.; Kay, L. E. *J. Am. Chem. Soc.* **2007**, *129*, 11468–11479.
(42) Kroenke, C.; Loria, J. P.; Lee, L. K.; Rance, M.; Palmer, A. G. *J. Am. Chem. Soc.* **1998**, *120*, 7905–7915.
(43) Trott, O.; Palmer, A. G., 3rd. *J. Magn. Reson.* **2002**, *154*, 157–160.
(44) Korzhnev, D. M.; Orekhov, V. Y.; Dahlquist, F. W.; Kay, L. E. *J. Biomol. NMR* **2003**, *26*, 39–48.
(45) Korzhnev, D. M.; Orekhov, V. Y.; Kay, L. E. *J. Am. Chem. Soc.* **2005**, *127*, 713–721.
(46) Nikolova, E. N.; Kim, E.; Wise, A. A.; O'Brien, P. J.; Andricioaei, I.; Al-Hashimi, H. M. *Nature* **2011**, *470*, 498–502.